Journal of Achievements in Materials and Manufacturing Engineering
VOLUME 41
ISSUES 1-2
July-August
2010

The analytical study on the optimal ballistic performance using interface theory

G.S. Hegde*, H.N. Narasimha Murthy, M. Krishna
Department of Mechanical Engineering, R V College of Engineering, Mysore Road, Bangalore- 560059, India
* Corresponding author: E-mail address: gagehe@yahoo.co.in

Received 18.04.2010; published in revised form 01.07.2010

Analysis and modelling

ABSTRACT

Purpose: Analytical determination of impact velocity for different combination of target and projectile materials is the objective of this paper.
Design/methodology/approach: The penetration efficiency is maximum when the interaction between the projectile and target is hydrodynamic. Considering zero strength for target and projectile the hydrodynamic impact velocities are predicted using hydrodynamic equation of state.
Findings: The hydrodynamic equation being an indeterminate equation is solved using interface theory (briefed in the appendix). The indeterminate Johnson-Cook (JC) model and Steinberg-Guinian (SG) model are also solved using interface theory to predict the influence of static strength of projectile and thermal softening effects. It is inferred that the penetration efficiency decreases with increasing static strength of target and also due to thermal softening of the projectile. In the process the plastic strain, the strain rate and the increase in temperature during impact are theoretically predicted. The segmented projectiles have less/more penetration efficiency than the monolithic impactors and hence require higher/lower impact velocities nearing to hydrodynamic state.
Research limitations/implications: The analytical results obtained are in fair agreement with experimental results obtained in the reviewed literatures. Some contrasts are also observed.
Originality/value: The paper present the analytical study on the optimal ballistic performance using interface theory.
Keywords: Hydrodynamic theory; Impact velocity; Interface theory; JC and SG models

Reference to this paper should be given in the following way:
G.S. Hegde, H.N. Narasimha Murthy, M. Krishna, The analytical study on the optimal ballistic performance using interface theory, Journal of Achievements in Materials and Manufacturing Engineering 41/1-2 (2010) 112-123.

1. Introduction

The The earlier analysis of long rod penetration had been based on steady-state hydrodynamic theory [1]. The target flow stress and the projectile strength are of negligible consequence at high velocities because of hydrodynamic nature of interaction. The Eichelberger [2] with shape charged jets confirmed the accuracy of hydrodynamic formulae at sufficiently high jet velocities. However at low velocities the strength of the targets, he experimentally showed, to be important and added strength term to the hydrodynamic equation. The experiments of Allen et al. [3] are important to highlight relatively less importance to projectile strength. Tate [4] and Alekseevskii [5] were successful

in modifying the theory to take into account the deceleration of the projectiles at low to moderate impact velocities. With the Eulerian hydrocode used in the works of Partrom [6] the penetration efficiency showed large variations with the changing flow stress of the penetrator. The hydrodynamic penetration efficiency with zero-strength penetrator is much more (20%) than highly strong penetrator.

The JC model [7] suits well for targets when strain rate dependence plays dominance. Both JC and SG models [8] used for the penetrators explained the mechanism with strain rate effect and thermal softening influences. Both of these models being indeterminate equations with more than two variables require the simulation to be carried out to study the influence of different variables. The belief that the penetration efficiency falls below that obtained from hydrodynamic theory is substantiated by Anderson, Jr. et al. [9] both theoretically and experimentally. They carried out the numerical simulation and experimentation with tungsten alloy as the projectile material and armor steel as the target materials.

The two dimensional numerical study by Rosenberg et al. [10] revealed the effect of strength of rod material, melting temperature and the plastic strain on the ballistic performance of long rod penetrator made of tungsten alloy impacting steel target. The investigation discussed the influence of mechanical softening and thermal softening mechanisms and the dominance played by them in reducing the penetration efficiency. The study of Yadav et al. [11] contradicted the made by Rosenberg and projected the influence of target material playing the dominant role in thermal softening. Yadav et al. studied computationally the tungsten heavy alloy (WHA) into 6061-T6, aluminum alloy using Lagrangian formulation. They studied strain hardening, strain rate hardening and thermal softening in both penetrator and target materials.

The recent studies off Dey et al. [12] confirmed more suitability of JC model to the ballistic penetration. The experiments conducted on specific target and penetrator materials showed good agreement with the simulated results using software codes.

Literatures [9-12], however conducted simulation and experimentation on monolithic projectiles. But investigations [13, 14] predicted better ballistic performance with segmented projectiles. Orphal et al. [13] and Holland et al. [14] concluded the dependency of the geometrical proportions of the segments on the penetration efficiency and provided different directions to the definition of penetration efficiency. Holland et al. provided the justification by experiments on segmented projectiles. However the results obtained from hydrocode helped in analysis of penetration mechanics of segmented and hybrid penetrators. The computer simulation of segmented penetrators by Daniel [15], gave the geometrical proportions of the segmented projectiles for satisfactory and better ballistic performance.

The hydrodynamic relation assuming steady state, incompressible, inviscid (zero-strength flow and conservation of momentum yields an expression with projectile indeterminate equation is solved using interface theory [16-19] as the computational tool. This expresses the penetration efficiency in terms of the projectile velocity. The ratio of mass density of the projectile and the target materials gives the square of the penetration efficiency. Hence the projectile velocity for hydrodynamic penetration is obtained.

The JC model is also an indeterminate equation with strain hardening and strain rate hardening and low stress as the variables. This is further solved optimally in terms of the static yield strength of the materials, using the interface theory, the original contribution of the authors. The SG model contains the penetration efficiency, total penetration depth and softening temperature as the variables. This also is an indeterminate equation that provides a suitable platform to apply the optimal interface theory.

Hedge et al. [16] and [17] successfully applied interface theory to solve the elasto-plastic equation distortion energy equation to optimize plastic strain and principal stresses respectively. Interface theory is the newly evolved computational tool that solves an infinite indeterminate equation to provide optimal (all positive rational values) interface variables in the n dimensional hyperspace.

In a segmented projectile the penetration efficiency depends on the mass density of the segments used. If the segments used are lower in density than the monolithic impactor the penetrator efficiency is lower than the monolithic penetrator and if higher density material is used for the segments the penetrator efficiency is higher, in which case hydrodynamic projectile velocity is lower. This fact is established by equating the kinetic energy of monolithic and segmented projectiles. However the geometric proportions of the segments used determines the effective densities of the segmented projectiles.

This paper focuses on the determination of the hydrodynamic impact velocities for different combination of projectile and target materials, computation of flow stress, plastic strain plastic strain rate, temperature increase and the penetration efficiency. This paper is organized to include brief survey of literature in the introduction, solution of the constitutional equations in formulation, results and discussion in implementation and highlight of the outcome in conclusions. The ready reference of interface theory is provided in the appendix.

2. Formulation

This section is organized to include the hydrodynamic equation for monolithic projectiles, the energy equation for the segmented projectiles, JC model for strength and SG model for thermal softening effect. The basic hydrodynamic equation is the indeterminate equation with projectile velocity, target speed and the penetration efficiency. The JC model with flow strength, strain hardening (plastic strain) and strain rate as the variables is also indeterminate. The SG model including flow stress, temperature increase and penetration efficiency can also considered to be indeterminate equation. These equations are solved optimally using interface theory (briefed in the appendix) for the respective variables in the equation. The energy equation for the segmented projectiles is solved directly for the penetration efficiency knowing the densities of the segments and hydrodynamic efficiency of the monolithic penetrator.

2.1. Hydrodynamic penetration

The projectile with density ρ_p moving with a velocity v_p hits a target that is moving with velocity u results in a penetration velocity v_t. During the interaction the projectile velocity is $(v_p - v_t)$.

Assuming the steady state penetration, the time dependent changes are neglected. For the hydrodynamic penetration it is necessary to assume the penetration to be incompressible, inviscid (zero strength for target and projectile) flow with steady state. By application of conservation of momentum at the projectile target interface, the following relation can be established:

$$\frac{1}{2}\rho_p(v_p - v_t)2 = \frac{1}{2}\rho_t v_t^2, \tag{1}$$

where ρ_t is the density of the target material. On simplification of equation (1),

$$2v_p v_t - v_t^2\left(1 - \frac{1}{\eta^2}\right) = v_p^2 \tag{2}$$

In equation (2) v_p is the only parameter known. For the time being, the material properties are assumed to be unknown. Hence,

$$\eta_m = \left(\frac{\rho_p}{\rho_t}\right)^{1/2} \tag{3}$$

The penetration efficiency is considered to be a variable. In equation (2) for maximum penetration velocity v_t has to be minimized and penetration efficiency (η_m) is to be maximized. The equation (2) is further modified to:

$$-z + 2v_p x = v_p^2 \tag{4}$$

$$z = v_t^2\left(1 - \frac{1}{\eta^2}\right) \text{ and } v_t = x \tag{5}$$

By the arrangement of equation (3) made suitable to apply the interface theory with the condition $a_{i-1} < a_i$ (the optimal interface theory requires the condition of arranging the coefficients of indeterminate equation in the ascending order)
The indeterminate equation (3) has:

$$a_i = [-1, 2v_p], \quad b = v_p^2 \quad \text{and} \quad X_i = [z, x]$$

Hence by interface theory applied to indeterminate equation (3) results in:

$$X_1 = z = \frac{v_p^2}{2v_p}\left(= \frac{b}{a_n}\right) = \frac{v_p}{2}$$

$$X_2 = x = \left[1 - \frac{a_1}{a_2}\right]\frac{b}{a_2} = \left[1 + \frac{1}{2v_p}\right]\frac{v_p}{2} = v_t \tag{6}$$

But from equation (3)

$$z = v_t^2\left(1 - \frac{1}{\eta^2}\right) = \frac{v_p}{2} \tag{7}$$

Substituting the value of v_t from formulation (6) in (7), it is arrived at:

$$\left[1 + \frac{1}{2v_p}\right]^2 \frac{v_p^2}{4}\left(1 - \frac{1}{\eta^2}\right) = \frac{v_p}{2} \tag{8}$$

On simplification of equation (8), it leads to:

$$\eta_v = \frac{(2v_p + 1)}{\left[(2v_p + 1)^2 - 8v_p\right]^{1/2}} \tag{9}$$

The equation (9) expresses the variable penetration efficiency (η_v) in terms of projectile velocity which is the only known with the assumption of zero strength for both projectile and the target. For a monolithic projectile in the hydrodynamic state, the condition assumed is:

$$\frac{\eta_v}{\eta_m} = 1 \tag{10}$$

But from equation (3), $\eta_m = \left(\frac{\rho_p}{\rho_t}\right)^{1/2}$

Simple manipulation of equations (9) and (10) leads to:

$$v_p = \frac{2\left(1 + 3\eta_m^2\right) \pm \sqrt{\left[4\left(1 + 3\eta_m^2\right)^2 - 16\left(\eta_m^2 - 1\right)\right]^2}}{8\left(\eta_m^2 - 1\right)} \tag{11}$$

The equation (11) gives the hydrodynamic penetration velocity when the material densities of the projectiles and the targets are known. Generally the hard-hard (tungsten projectile and armor steel target), hard to soft (steel to aluminum), soft to soft (copper to aluminum) combinations of interaction are observed in practice. The saturation impact velocities obtained from equation (11) is the lower bound estimation for the impact velocities of the projectile. The upper bound velocity limit is to be estimated based on the strength of the projectile and the target as well as the temperature rise in the interaction. Higher strength for the target requires higher velocity and higher strength for the projectile requires lower velocities. Hence a balance is to be struck to achieve optimum saturation velocity or the impactor.

2.2. Geometrical proportion

For the designers to determine the length L, to diameter (D) ratio of the penetrator the parameters known are the density of the material of the target and the penetration efficiency, assumed to vary 20% from the hydrodynamic efficiency of penetration. The variation is justified by the consideration of finite strength for the target and the projectile material. By definition:

$$\left(\frac{\rho_p}{\rho_t}\right)^{1/2} = \eta$$

But $$\rho_p = \frac{m}{\pi D^2 L} = \frac{m}{\pi D^3}\left(\frac{D}{L}\right) = \eta^2 \rho_t \quad (12)$$

From equations () and () the following relation is arrived at:

$$-\rho_t\left(\frac{L}{D}\right) + \frac{1}{\pi\eta^2}\left(\frac{m}{D^3}\right) = 0 \quad (13)$$

The equation (13) is of the form given by:

$$a_1 x + a_2 y = 0, \quad (14)$$

where $a_i = \left[-\rho_t, \frac{1}{\pi\eta^2}\right]$,

$X_i = [x, y] = \left[\frac{L}{D}, \frac{m}{D^3}\right]$ and $b = 0$

Hence by the application of interface theory:

$$x = \left(\frac{L}{D}\right) = \frac{1}{a_n} = \pi\eta^2 \quad (15)$$

$$y = \frac{m}{D^3} = -\frac{a_1}{a_2}\left(\frac{1}{a_2}\right) = \rho_t\left(\pi\eta^2\right)^2 \quad (16)$$

For a penetrator of tungsten heavy alloy (WHA) and the steel target (RHA) the L/D ratio is 6.88 (Table-1).

2.3. Segmented projectiles

A monolithic projectile is simply a cylindrical rod made with single main material. But a segmented projectile is also a cylindrical rod where main material is separated by spacers made of another material. If in a segmented projectile L_1 is the total length of the main material and L_2 is the total length of secondary spacers the length of the projectile is as follows:

$$L_p = L_1 + L_2 \quad (17)$$

Ratio of the lengths of main material to the length of projectile is given as:

$$m = \frac{L_1}{L_p} = \frac{L_1}{L_1 + L_2} \quad (18)$$

The ratio of spacers to the total length of the projectile is formed as:

$$n = \frac{L_2}{L_p} = \frac{L_2}{L_1 + L_2} \quad (19)$$

Let mm and v_m be the mass and velocity of monolithic projectile respectively. Assume that ms and v_s to be respective mass and velocities of segmented projectile. Equating the kinetic energies of the two:

$$\frac{1}{2} m_m v_m^2 = \frac{1}{2} m_s v_s^2 \quad (20)$$

$$v_s = \sqrt{\frac{m_m}{m_s} v_m^2}$$

$$v_s = \sqrt{\frac{\rho_m L_p}{m\rho_m L_p + n\rho_s}} v_m \text{ and}$$

$$v_s = \sqrt{\frac{\rho_m}{m\rho_m + n\rho_s}} v_m \quad (21)$$

v_m is the hydrodynamic saturation velocity of the monolithic projectile. v_s is hydrodynamic velocity of the segmented projectile.

If $\rho_m > \rho_s$ then $v_s > v_m$

If $\rho_m < \rho_s$ then $v_s < v_m$

Hence from equation (9) and (16) the velocity of the segmented projectile has the form:

$$v_s = \left[\frac{2\left(1+3\eta_m^2\right) \pm \sqrt{4\left(1+3\eta_m^2\right)^2 - 16\left(\eta_m^2 - 1\right)^2}}{8\left(\eta_m^2 - 1\right)}\right] \sqrt{\frac{\rho_m}{\left(m\rho_m + n\rho_s\right)}} \quad (22)$$

The equation (22) predicts lower bound limit on the estimation of the hydrodynamic velocity of the segmented projectiles. When the density of main material is greater than spacer material hydrodynamic efficiency is less than the monolithic projectile and when density of spacer material is greater than primary material the hydrodynamic efficiency of segmented projectile is more than monolithic. The cross- section of both monolithic and segmented projectiles is considered equal.

2.4. JC Model

The phenomenological constitutive relation for flow stress in target materials proposed by Johnson and Cook [7] has been frequently used in impact mechanics. This model provides results in good agreement with experiment in narrow dynamic range. The model establishes relation between flow stress and the strain rate:

$$\sigma_{eq} = f\left(\varepsilon_{eq}, \dot{\varepsilon}^{*}, \sigma_0\right) \tag{23}$$

The simplified expression for equation (23) is as follows:

$$\sigma_{eq} = \sigma_0\left(1 + A\varepsilon_{eq}^{n}\right)\left(1 + C\ln\dot{\varepsilon}^{*}\right) \tag{24}$$

The constants σ_0, A, C, and n, in the relation (24), are listed as in Table-3.

$$\dot{\varepsilon}^{*} = \left(\frac{\dot{\varepsilon}}{\dot{\varepsilon}_{ref}}\right) \tag{25}$$

The expansion of the equation (24) results in an indeterminate equation with ε_{eq} and σ_{eq}, as the variables to be determined. Such an equation is of the form:

$$\sigma_{eq} = \sigma_0 + A\sigma_0\varepsilon_{eq}^{n} + C\sigma_0\left(\ln\dot{\varepsilon}^{*}\right) + AC\sigma_0\varepsilon_{eq}^{n}\left(\ln\dot{\varepsilon}^{*}\right) \tag{26}$$

For any given material (refer Table-3) $A>C$ and the following cases hold.
Case A: when A, C are less than 1, $AC<C<A<1$
Case B : when A and C are greater than 1, $1<C<A<AC$
Case C: when A>1 and C<1, it can be $C<AC<1<A$

For the preceding three cases, the analysis using optimal interface theory can be presented as following.

Case A:
The hard materials like tungsten (WHA) and 4340 steel (RHA) fall in this category. The equation (21) in form useful to apply interface theory with ascending order of the coefficients, is given as:

$$\sigma_0 = -(AC\sigma_0)\varepsilon_{eq}^{n}\left(\ln\dot{\varepsilon}^{*}\right) - C\sigma_0\left(\ln\dot{\varepsilon}^{*}\right) - A\sigma_0\varepsilon_{eq}^{n} + \sigma_{eq} \tag{27}$$

In the equation (27) as compared with equation (A1) of appendix it shows:

$$a_i = \left[(-AC\sigma_0), (-C\sigma_0), (-A\sigma_0), 1\right]$$

$$X_i = \left[\left(\varepsilon_{eq}^{n}\dot{\varepsilon}^{*}\right), \left(\ln\dot{\varepsilon}^{*}\right), \varepsilon_{eq}^{n}, \sigma_{eq}\right]$$

$$b = \sigma_0$$

Now by the application of the optimal interface theory:

$$X_1 = \varepsilon_{eq}^{n}\left(\ln\dot{\varepsilon}^{*}\right) = \frac{b}{a_n} = \frac{\sigma_0}{1}$$

$$X_2 = \left(\ln\dot{\varepsilon}^{*}\right) = \left[1 - \frac{a_1}{a_2}\right]\frac{b}{a_n} = [1 - A]\sigma_0 \tag{28}$$

$$X_3 = \varepsilon_{eq}^{n} = \left[1 - \frac{a_2}{a_3}\right]\frac{b}{a_n} = \left[1 - \frac{C}{A}\right]\sigma_0$$

$$X_4 = \sigma_{eq} = \left[1 - \frac{a_3}{a_4}\right]\frac{b}{a_n} = [1 + A\sigma_0]\sigma_0$$

Case B:
This type of behavior is evidenced in the materials like gold and aluminum. The equation of the form (26) made suitable for the application of interface theory optimizing the variables to get all positive values, has the form:

$$\sigma_0 = -(C\sigma_0)\left(\ln\dot{\varepsilon}^{*}\right) - (A\sigma_0)\varepsilon_{eq}^{n} - (AC\sigma_0)\varepsilon_{eq}^{n}\left(\ln\dot{\varepsilon}^{*}\right) + \sigma_{eq} \tag{29}$$

This gives a comparison with the equation (A1) of the appendix.

$$a_i = \left[(-C\sigma_0), (-A\sigma_0), (-AC\sigma_0), 1\right]$$

$$X_i = \left[\left(\ln\dot{\varepsilon}^{*}\right), \varepsilon_{eq}^{n}, \varepsilon_{eq}^{n}\left(\ln\dot{\varepsilon}^{*}\right), \sigma_{eq}\right]$$

$$b = \sigma_0$$

From Interface theory it leads to the solution as:

$$X_1 = \sigma_0 = \left(\ln\dot{\varepsilon}^{*}\right)$$

$$X_2 = \varepsilon_{eq}^{n} = \left[1 - \frac{a_1}{a_2}\right]\sigma_0 = \left[1 - \frac{C}{A}\right]\sigma_0$$

$$X_3 = \varepsilon_{eq}^{n}\left(\ln\dot{\varepsilon}^{*}\right) = \left[1 - \frac{a_2}{a_3}\right]\sigma_0 = \left[1 - \frac{1}{C}\right]\sigma_0 \tag{30}$$

$$X_4 = \sigma_{eq} = [1 + AC\sigma_0]\sigma_0$$

Case C:
The soft materials like copper exhibited the behavior of this type. The values of A and C are such that the equation (26) gets arranged to the form:

$$\sigma_0 = -C\sigma_0\left(\ln\dot{\varepsilon}^*\right) - AC\sigma_0\varepsilon_{eq}^n\left(\ln\dot{\varepsilon}^*\right) - A\sigma_0\varepsilon_{eq}^n + \sigma_{eq} \quad (31)$$

Comparing this equation with that of appendixed equation (A1):

$$a_i = [(-C\sigma_0),(-AC\sigma_0),(-A\sigma_0),1]$$
$$X_i = \left[\left(\ln\dot{\varepsilon}^*\right),\varepsilon_{eq}^n\left(\dot{\varepsilon}^*\right),\varepsilon_{eq}^n,\sigma_{eq}\right]$$
$$b = \sigma_0$$

The optimal interface theory is now exercised on equation (26) to yield the solution in the following way:

$$X_1 = \left(\ln\dot{\varepsilon}^*\right) = \sigma_0$$
$$X_2 = \varepsilon_{eq}^n\left(\ln\dot{\varepsilon}^*\right) = \left[1 - \frac{a_1}{a_2}\right]\frac{b}{a_4} = \left[1 - \frac{1}{A}\right]\sigma_0$$
$$X_3 = \varepsilon_{eq}^n = \left[1 - \frac{a_2}{a_3}\right]\frac{b}{a_4} = [1 - C]\sigma_0$$
$$X_4 = \sigma_{eq} = \left[1 - \frac{a_3}{a_4}\right]\frac{b}{a_4} = [1 + A\sigma_0]\sigma_0 \quad (32)$$

From the solutions (28), (30) and (32), it is concluded that with the increase in static strength of the target materials there is increase in plastic strain, strain rate and equivalent flow stress irrespective of the hardness of the target materials. The interface theory used as the optimization tool correctly predicts the behavior of the target materials in the impact analysis of the projectiles. This observation reveals deviation of the penetration efficiency from the hydrodynamic penetration behavior, due to the influence of non-zero strength of the target materials.

2.5. Steinberg-Guinian (SG) model

The behavior of the penetrator materials is well predicted by the empirical relation suggested by Steinberg and Guinian [8]. The influencing variables in the SG model are the equivalent flow stress, static yield strength, penetrator efficiency, and the increase in temperature. The functional relation for the SG model is:

$$\sigma_{eq} = f(\sigma_0, \Delta T, \eta) \quad (33)$$

The equation (28) in the expanded form is the indeterminate equation of the type:

$$\sigma_{eq} = \sigma_0\left[1 + S_1(T - T_0) + S_2(\eta)^{1/3}P\right] \quad (34)$$

In equation (29) S_1, irrespective of the material is always negative [9] and S_2 is always less than one. The rearrangement of the equation (29) turns to the form as:

$$\sigma_0 = -S_2(\eta)^{1/3}P\sigma_0 - S_1(T - T_0)\sigma_0 + \sigma_{eq} \quad (35)$$

The comparison of equation (30) with that of the indeterminate system (A1) of the appendix lays plat form to arrange known and unknowns as:

$$a_i = [(-S_2\sigma_0),(-S_1\sigma_0),1]$$
$$X_i = \left[(\eta)^{1/3}P,(T - T_0),\sigma_{eq}\right]$$
$$b = \sigma_0$$

The arrangement of a_i's in the ascending order opens up a situation to apply optimal interface theory leading to the solution:

$$X_1 = (\eta)^{1/3}P = \sigma_0$$
$$X_2 = (T - T_0) = \left[1 - \frac{a_1}{a_2}\right]\frac{b}{a_3} = \left[1 - \frac{S_2}{S_1}\right]\sigma_0$$
$$X_3 = \sigma_{eq} = \left[1 - \frac{a_2}{a_3}\right]\frac{b}{a_3} = [1 - S_1\sigma_0]\sigma_0 \quad (36)$$

The negative value to the S_1 in solutions (36) makes two things clear: 1. the temperature in the interaction increases with increase in the static strength, 2. there is increase in the equivalent flow stress with the increase in the target material strength. The solution X_1 is a non linear relation between the penetration depth and the efficiency, which is solved optimally after transforming to the linear form as:

$$-P + \frac{\sigma_0}{(\eta)^{1/3}} = 0 \quad (37)$$

Interface theory with the case b=0 applied to equation (37) yields:

$$\frac{1}{(\eta)^{1/3}} = \left(-\frac{a_1}{a_2}\right)\frac{1}{a_n} = \left(\frac{1}{\sigma_0}\right)\frac{1}{\sigma_0}$$

$$\eta = \sigma_0^6 \tag{38}$$

This gives the lower bound on the penetration depth *(P)* and efficiency. To consider upper bound solution the linear form of non-linear equation suitable is:

$$-(\eta)^{1/3} + \frac{\sigma_0}{P} = 0 \tag{39}$$

This, from interface theory leads to the solution:

$$(\eta)^{1/3} = \frac{1}{\sigma_0} \text{ or } \eta = \left(\frac{1}{\sigma_0}\right)^3$$

$$\frac{1}{P} = \left(\frac{1}{\sigma_0}\right)^2 \text{ or } P = (\sigma_0)^2 \tag{40}$$

The solution (40) is more useful result from the common understanding of penetration behavior. Here two things are very clear: 1. The total penetration depth increases with increase in static strength of the materials for a given target material, 2. From the definition, the penetration efficiency is the ratio of depth of penetration to the consumed length, which decreases with increase in static strength because of increasing consumed length. In this process the penetration mechanism gets optimized for penetration efficiency and depth of penetration.

The numerical results of the preceding theoretical deliberation signify that the JC model is suitable for all metals except for the metals of the type of aluminum. The SG model predicts well the mechanism of penetration of hard metals like tungsten and steel (RHA). But SG model provides positive increase in temperature in the penetration process irrespective of projectile materials.

3. Computational analysis

3.1. Results of Hydrodynamic penetration

To understand the importance of feel for numbers in the theoretical deliberations in section (2), the following examples of implementation are demonstrated. The material properties and the values of the constants are extracted from the reference [20]. The computational results for the hydrodynamic velocities for projectile and target materials in different interaction of penetration process are listed in Table 1. The variation of hydrodynamic penetration efficiency against the projectile velocity is plotted in Figure 1. L/D ratio for penetrators is shown in Figure 2.

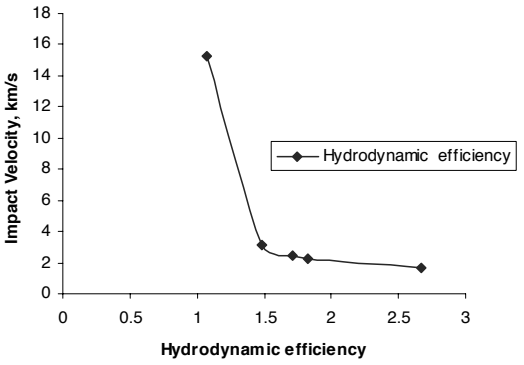

Fig. 1. Hydrodynamic efficiency versus impact velocity

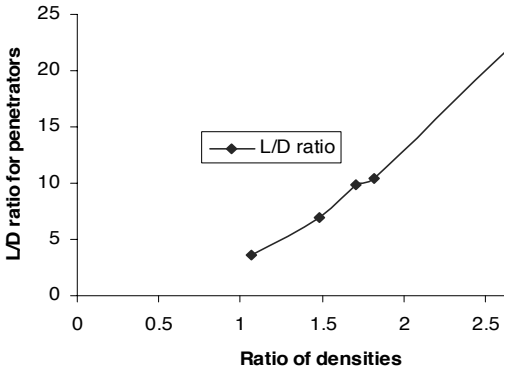

Fig. 2. L/D ratio for penetrators

It is evident from Table 1 that, as the difference between the projectile density and the target material decreases there is need for higher projectile velocity for penetration. Anderson et al. [20] computed for tungsten-steel interaction, an impact velocity of 3.1 km/s and 2.495 km/s for copper projectile and aluminum target interaction. This gives a justification to the results in Table 1. The plot Figure 1 shows that the impact velocity bears a non-linear variation with the hydrodynamic efficiency. However the experimental works [20] provided maximum penetration with impact velocities 3.07 km/s for tungsten projectile and steel target, and 2.5 km/s for copper projectile and aluminum target interaction. The respective velocities 3.09 km/s and 2.25 km/s as computed in Table 1, are in close agreement with the experimentation results in [20].

3.2. Numerical results for segmented projectiles

The computations are carried out for the combination of various primary and the spacer materials and length ratios using equation (21). The impact velocities and the penetration efficiencies for different combination of materials and length ratios are listed in Table 2. And variation of impact velocity

against length ratio is plotted. The hard-hard material combination (steel as main material and tungsten as the spacer material) and soft-hard combination (copper as main material and tungsten as spacer material) are tried and results are tabulated. The equation (21) allows the combination of any two materials with known densities and proportions. The plot of the results in Figure 3 depicts that the saturation impact velocity increases with the increase in the density and spacer length. But the change is less prominent in the change of spacer length for a given material for the spacer. With spacer material denser than the monolithic projectile materials same as main material the velocity of impact needed is 10% less. For a lighter material used for spacer the effect is opposite.

a)

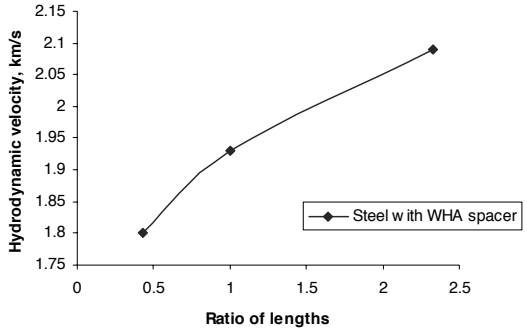

b)

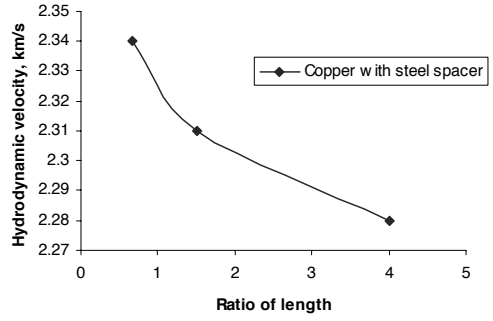

Fig. 3. Hydrodynamic velocity for segmented projectiles: a) Steel with WHA spacer, b) Copper with steel spacers

3.3. Computational results with JC model

In case of hard target metals like steel and tungsten the plastic strain is higher than negligibly small equivalent plastic strain in softer metals for target due to the fact that softer metals deform more than the harder metals. The strain rate also increases with increase in static yield strength. One observation from Table 3 reveals that the flow stresses increase with the increase in the static strength of the used materials. The high values of A=125 and C=6.52 [20] for the aluminum the flow stress is very high as for materials like aluminum and gold are attributed to the fact that they have high A values and low static yield strengths. In the results of Table 3 reference strain rates of 1.0 1/s is assumed. The JC model predicts very well the behavior of the targets made of steel, tungsten, copper and gold. But with aluminum the observations are different with the JC analytical model.

3.4. Computational results of SG model

From the optimization through interface theory applied to SG model (more suitable to penetrators) the flow stress (σ_{eq}), the temperature rise (ΔT) and the optimum penetration efficiency (η) along with total depth of penetration (P) for the projectile materials are computed as indicated in Table 4. The constants taken from [20] are used in the computation and are listed along with the results in Table 4.

In high strength penetrators like tungsten (WHA) and steel (RHA) the temperature rise is considerable. In these the penetration efficiency is relatively low but the total depth of penetration is high. In case o soft metals with low static yield strength the temperature rise is somewhat lower, but the efficiency is exorbitantly high for which the justification fails. The flow stress in all these cases is slightly more than the static yield strength. For the denser material like gold with low static strength the temperature rise in the interaction is less but the efficiency is very high. Hence the SG model fails to explain the penetration of the materials with less static strength. However from the plot in Figure 4 for RHA and WHA the observations are quite justified.

Table 1.
Summary of calculation of projectile velocity

Projectile materials	Density of projectiles (gm/cm^3)	Target materials	Density of target materials (gm/cm^3)	Hydro-dynamic efficiency	Projectile velocity	L/D
Tungsten	17.1	Steel	7.85	1.48	3.09	6.9
Steel	7.85	Aluminum	2.7	1.71	2.43	9.18
Copper	8.93	Aluminum	2.7	1.82	2.25	10.4
Gold	19.24	Aluminum	2.7	2.67	1.67	22.4
Copper	8.93	Steel	7.85	1.07	15.21	3.6

Table 2.
Results for segmented projectiles

Main matl.	Spacer matl.	m	n	m/n	v_s	n_s
Steel	Tungsten	0.3	0.7	0.43	1.8	1.77
		0.5	0.5	1.0	1.93	1.7
		0.7	0.3	2.33	2.09	1.63
Copper	Steel	0.4	0.6	0.67	2.34	1.54
		0.6	0.4	1.5	2.31	1.55
		0.8	0.2	4.0	2.28	1.56

Table 3.
Results for JC model

Target materials	σ_0	A (GPa)	C	n	ϵ_{eq}	$\dot{\varepsilon}$ x10^6	σ_{eq}
Tungsten	1.507	0.117	0.016	0.12	8.95	3.78	1.77
RHA	0.793	0.643	0.014	0.26	0.376	1.33	1.2
Aluminum	0.324	125	6.52	0.1	7.5e-6	1.38	85.87
Gold	0.02	49	3.75	0.39	3.6e-5	1.02	0.094
Copper	0.0897	3.26	0.025	0.31	3.9e-4	1.09	0.116

Table 4.
Results for SG model

Projectile materials	σ_0	$(-S_1)$	S_2	$(T-T_0)$	σ_{eq}	n	Pxe2
Tungsten	1.507	1.52e-4	0.01	100.7	1.5073	0.292	2.27
RHA	0.793	1.4e-4	0.0103	59.54	0.7931	2.005	0.63
Aluminum	0.324	6.52e-2	6.16	30.61	0.3313	29.4	0.104
Gold	0.02	3.75e-2	3.11	1.7	0.02	125e3	0.0004
Copper	0.0897	2.5e-4	0.0109	4.0	0.0897	13.9e2	8.04e-3

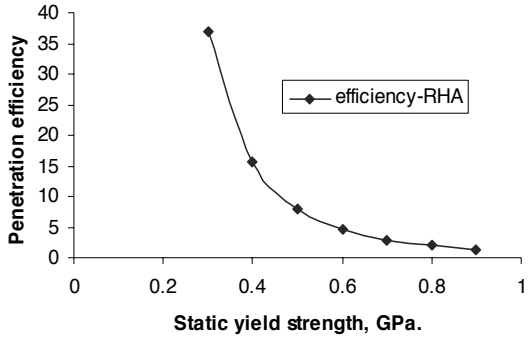

Fig. 4. Variation of efficiency against static strength- RHA steel

4. Discussions

The theoretical and experimental investigations conducted with penetration of tungsten rod (WHA) into steel targets [20] at impact velocity 2.085 km/s gave lower penetration efficiency of 1.2, but for the impact velocity at 3.1 km/s it goes very close to 1.5. In this paper it is computed to obtain the penetration velocity of 3.09 km/s for the penetration efficiency of 1.48. When tungsten is used as spacer material with steel as primary metal for varied spacer lengths the efficiency showed variation from 1.77 to 1.63 while the penetrator impact velocity varied from 1.8 to 2.1. The JC model for a steel target in paper [12] predicted, both theoretically and experimentally, an equivalent strain of 0.4 or an equivalent stress of 0.8 GPa. The current paper in this effort (Table 3) computed a strain of 0.376 for an optimal equivalent stress of 1.2 GPa. But it may be noted that SG model in Table 4 gives an equivalent stress of 0.793 GPa., for a strain of 0.4 which agrees with the result of reference [12]. This paper as in Table 4 predicted for a strain of 0.4 and stress 0.793 GPa., a temperature rise of 60^{o}C, but in reference [12] similar temperature rise is reported at the equivalent stress of 0.4 GPa., which is lower than 0.8 GPa.

The experimental and theoretical findings of [20] considered 3.115 km/s as the penetration velocity for gold rod into aluminum targets for which the penetration efficiency is closely around 2.7. But in this paper a hydrodynamic saturation velocity (Table 1) of 1.67 km/s is computed for an efficiency of 2.67, which is also the ratio of densities. The velocity higher by 10-15 % of 1.67 km/s is more justified than 3.115 km/s. The results of [20] however match closely with the computational results of this paper for the penetration of copper into aluminum targets. In [20] the velocity was 2.495 km/s for the efficiency of 1.8. This effort optimally computed 2.25 km/s as the velocity for a hydrodynamic efficiency of 1.82. However the reference [20] for the penetration of steel into aluminum target used an impact velocity of 3.91 km/s or an efficiency of 1.7. But from the graphs [20] the impact velocity of 2.43 km/s as obtained in this paper is more justified to get efficiency of 1.71. The plots reported in [20] for experimental workouts cross the hydrodynamic curve (a horizontal line) at a point giving the data for impact velocity and the efficiency.

The data at these intersections closely match with the theoretical and optimal findings (Table 1) in this paper. The results of Table 1 are for the hydrodynamic state. But the results in Table 4 are indicatives of the fact that the static strengths of the target and projectile have the influence on the practical impact velocities and the corresponding penetration efficiency. For the hydrodynamic penetration the velocity needed is more than the saturation velocities. Typical values for RHA steel may be noted in Table 4. The flow stress in target is considerably higher than the static yield strengths as provided in Table 3. But equivalent flow stresses in Table 4 for penetrators are marginally higher than the static strengths. Table 3 reveals that strain rate decreases with the decrease in density of the target materials. But the behavior is complex by the contribution of other factors. The variations in parameters like plastic strain, strain rate and depth of penetration have direct relation with static yield strength variations in given materials. The JC model predicts favorably the behaviors of the targets like rolled homogeneous armor (RHA) steel, copper and gold. As per the observations by SG model in this paper the steel, tungsten and aluminum are suitable as the projectile materials. The results of aluminum are reasonably acceptable.

The properties needed to calculate the hydrodynamic efficiency, are the densities of the projectile and the target materials. The Figure 1 obtained to from equation (9) is useful in predicting the lower bound on hydrodynamic penetration efficiency of the projectiles considering the zero static strength. For the segmented projectiles with steel as the main material and tungsten as the segment the penetration velocity varies in the range (Figure 3) 1.8 km/s to 2.1 km/s. But for copper steel combination the curve is flat varies closely around 2.3 km/s. The Figures (4-9) depict the variation of plastic strain, the flow stress, penetration efficiency, the temperature rise, strain rate and the total depth of penetration for RHA steel. The static strength is varied in the range of 0.2 to 0.9 for varying hardness of the material. Plastic strain varies parabolically while strain rate varies linearly. The penetration efficiency decreases hyperbolically with increase in static strength of RHA steel. But the variation of equivalent low stress is non-linear. The increase in temperature rise is linear with the increase in the static strength. However the total depth of penetration increases parabolically with increase in the static yield strength. The results in this analytical deliberation appear to be realistic and go well with the common observations and understandings.

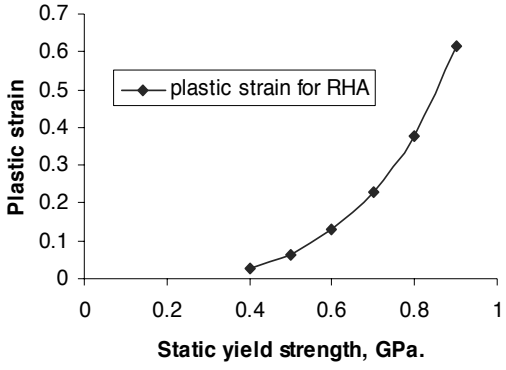

Fig. 5. Variation of plastic strain against static yield strength for RHA

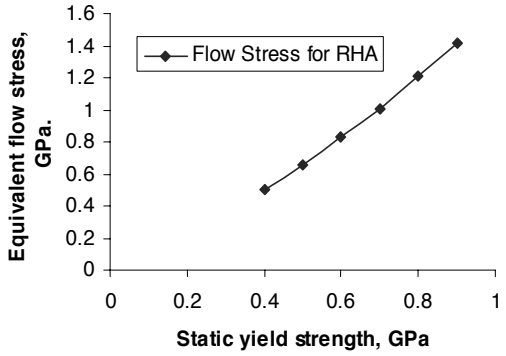

Fig. 6. Variation of flow stress against flow stress for RHA steel

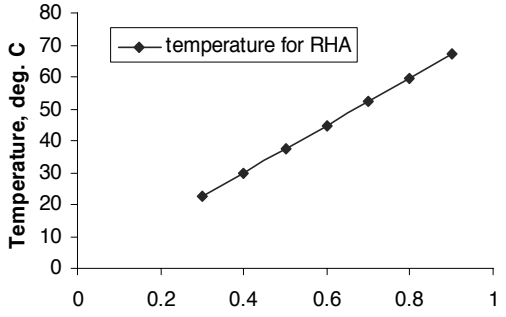

Fig. 7. Variation of temperature against static strength for RHA

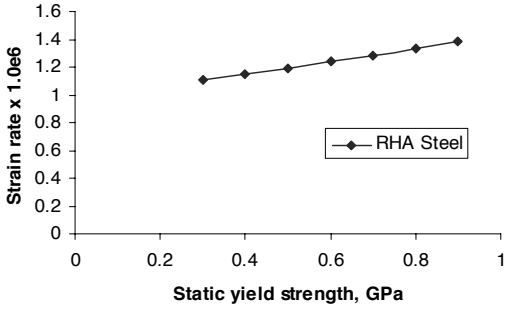

Fig. 8. Variation of strain rate against static strength for RHA Steel

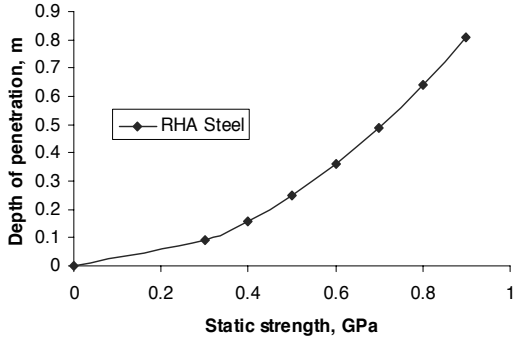

Fig. 9. Variation of depth of penetration for RHA steel

5. Conclusions

The real time penetration of the projectile into a target is a complex process, involving several variables. The reality has to be approached through idealization. Hydrodynamics theory with the consideration of zero static strength is the first step in the process. The hydrodynamic theory is transformed into an indeterminate equation and optimally solved using interface theory to express the saturation projectile velocity in terms of efficiency which is obtained from the density of the projectile and targets. In the ballistic penetration process the known parameters are the densities of the projectile and the targets. The static yield strengths of both are approximately known. In real situation the information about the target is unknown. In such a situation the hydrodynamic impact velocity can be predicted as outlined in this paper. The JC and the SG models are the experimentally derived explicit relations in terms of static strength, flow stress, plastic strains, and the strain rate, total depth of penetration, the temperature rise and the penetration efficiency. Because of the presence of the more unknown parameters than the equations available to solve, the two models result in indeterminate equations that are solved using the optimal interface theory. The results obtained in this paper show some comparisons that are similar and contrasting with the theoretical and experimental results of the published investigations in the reviewed literatures. Interface theory is used here as the computational analysis tool to predict optimal vector (all positive) in the 'n' dimensional hyperspace. For the quick and brief reference of the interface theory short explanation is provided in the appendix. The authors honestly presume that the outcome of this paper should be of good use to the ballistic community.

Appendix: (Brief of the Interface theory)

A general linear indeterminate equation in an 'n' dimensional hyperspace for the proof of the optimal interface theory, be

$$\sum_{i=1}^{n} a_i X_i = b \tag{A1}$$

a_i are the coefficients of different terms in equation (A1) and b is the output of a system governed by equation (A1) with X_i as the unknown interface variables. For the simple understanding of the proof of interface theory the specific form of indeterminate equation (A1) with three variables is considered as:

$$a_1 X_1 + a_2 X_2 + a_3 X_3 = b \tag{A2}$$

After separating out the segment, $a_2 X_2 + a_3 X_3 - b = V_1$,

we have the equation of the form presented in the following way:

$$a_1 X_1 + V_1 = 0 \tag{A3}$$

The equation (A3) is also an indeterminate equation with two variables that have infinite solutions. The handle roots for (A3) are:

$$(X_1, V_1) = (1, -a_1)$$

But it is the proportionating adapter h that induces the infinity in the solution to equation (A3) as:

$$(X_1, V_1) = (h, -a_1 h)$$

The interface adaptor h is kept as the variable till the final segmentation in which it is estimated as the ratio of the output and the coefficient of the last term that is the maximum of all. By this way the optimal vector containing all positive value of interface variables is arrived at.

With the segmentation of (A3) the following indeterminate equation is obtained as:

$$a_2 X_2 + V_2 = -a_1 h \tag{A4}$$

The solutions to equation (A4) are:

$$(X_2, V_2) = \left[\left(1 - \frac{a_1}{a_2}\right)h, -a_2 h\right]$$

In the final segmentation of (A2) leading to the equation:

$$a_3 X_3 + V_3 = -a_2 h \tag{A5}$$

The roots of the equation (A5) are given as:

$$(X_3, V_3) = \left[\left(1 - \frac{a_2}{a_3}\right)h, -a_3 h\right]$$

But $V_3 = -b = -a_3 h$

Hence the interface adapter for the equation (A2) takes the value:

$$h = \frac{b}{a_3}$$

But for the equation in general (A1) the interface adapter with the logical way is:

$$h = \frac{b}{a_n}$$

Finally this leads to the generation of roots in the form:

$$X_i = \left(1 - \frac{a_{i-1}}{a_i}\right)\frac{b}{a_n} \qquad \text{for } i = 1 - n \tag{A6}$$

In solution (A6) if b = 0 all values become zero. Hence in equation (A5) V_3 is initialized to 1 with the solution becoming evaluated to the type:

$$(X_3, V_3) = \left[-\frac{a_2}{a_3} h, (1 - a_3 h) \right]$$

But the final term $V_3 = 0$

Hence the interface adapter is $h = \frac{1}{a_3}$

The validity may be cross-verified by the back substitution. *So* when $b = 0$ the solutions to *Xi* are:

$$X_i = \left(1 - \frac{a_{i-1}}{a_i}\right)\frac{1}{a_n} \qquad i = 1 - (n-1)$$

$$X_n = \left(-\frac{a_{n-1}}{a_n}\right)\frac{1}{a_n} \qquad i = n \qquad \text{(A7)}$$

Since the equations (A4) and (A5) are the segments of equation (A3) the interface adapter h can not assume different values but one unique value as estimated. If the equations are individually different the h can take any or different values. The validity of the solutions (A6) and (A7) can be verified by substitution into equation (A1).

For positive values of b all the solutions are positive when:

$$\left(1 - \frac{a_{i-1}}{a_i}\right) > 0$$

This condition is achieved only if $a_{i-1} < a_i$.

Hence the arrangement of the coefficients in the ascending order the solutions obtained are optimal and positive. This is the necessary and sufficient condition of optimization in interface theory. The solutions of both the type (A6) and (A7) are used in this paper to optimally solve the indeterminate equations derived from hydrodynamic theory, JC model and SG model.

References

[1] G. Birkhof, D.P. MacDougall, E.M. Pugh, G. Taylor, Explosives with lined cavities, Journal of Applied Physics 19 (1948) 563-582,.

[2] R.J. Eichelberger, Experimental test of theory of penetration by metallic jets, Journal of Applied Physics 27/1 (1956) 63-68.

[3] W.A. Allen, J.W. Roger, Penetration of a rod into a semi-infinite target, Journal of the Franklin Institute 272 (1961) 275-284.

[4] A. Tate, A theory for the deceleration of long rod after impact, Journal of the Mechanics and Physics of Solids 15 (1967) 387-399.

[5] V.P. Alekseevskii, Penetration of a rod into a target at high velocity, combustion and expansions and shok-waves (translated from Russian), NewYork: Faraday Press, 2, 1987, 63-66.

[6] Y. Patrom, D. Yaziv, High pressure science and technology, AIP Press, New York, 1994.

[7] G.R. Johnson, W.H. Cook, A constitutive model and data for metal subjected to large strain, high strain rate, temperatures and pressures, Proceedings of the 7th International Symposium On ballistics, The Neherland: Hague, pp. 541-547, 1983.

[8] D.J. Stienberg, Equation of state and strength properties of selected materials, UCRL-MA-106439, Livermore, CA, Lawrence Livermore National Laboratory, Feb. 1991.

[9] J.E.,Jr. Anderson, J.D. Walker, An analytical expression for P/L for WA rods into armor steel, In: Schimidt SC, Tao WC, editors. Shock comperession in condensed matter 1995 Woodbury, NY: AIP press, 1996, 1135-1138.

[10] Z. Roseberg, E. Dekel, The relation between penetration capability of long rods and their length to diameter ratio, International Journal of Impact Engineering 15/3 (1998) 283-296.

[11] S. Yadav, E.A. Reppetto, G. Ravichandran, M. Ortiz, A computational study of the influence of thermal softening on ballistic penetration in metals, International Journal of Impact Engineering 25 (2001) 787-803.

[12] S. Dey, T. Borvik, O.S. Hopperstad, M. Langseth, On the influence of constitutive relation in projectile impact of steel plates, International Journal of Impact Engineering 34 (2007) 464-486.

[13] D.L. Orphal, R.R. Franzen, Penetration Mechanics and performance of segmented rod against metal targets, International Journal of Impact Engineering 10 (1990) 427-438.

[14] P.H. Holland, J.T. Gordon, T.L. Menna, A.C. Charters, Hydrocode results for the penetration of continuous, segmented and hybrid rods compared with ballistic experiments, International Journal of Impact Engineering 10 (1990) 241-250.

[15] R.S. Daniel, 2D computer simulation of segmented penetrators impacting semi-infinite steel targets, International Journal of Impact Engineering 9/1 (1990) 35-43.

[16] Ganesh S. Hegde, G.M. Madhu, Enhaced explicit scheme to solve transient heat conduction problem, Chemical Product and Process Modeling 2/1 (2007) art. 4

[17] Ganesh S. Hegde, G.M. Madhu, , Hegde's ultimate numerical technique (HUNT) for steady state diffusion problem, Chemical Product and Process Modeling 2/3 (2007) art. 5

[18] Ganesh S. Hegde, J. Shiv Prasad, R. Sridhar, Interface driven optimization of springback in stretch bending of autobody panels, Archives of Computational Materials Science and Surface Engineering 1/3 (2009) 168-173.

[19] Ganesh S. Hegde, J.R. Nataraj, R. Sridhar, Hegde's instability mechanics for predicting forming limits in sheet metal forming, Archives of Computational Materials Science and Surface Engineering 1/3 (2009) 155-160.

[20] C.E.,Jr., Anderson, D.L. Orphal, R.R. Franzen, J.D. Walker, On the hydrodynamic approximation for long rod penetration, International Journal of Impact Engineering 22 (1999) 23-43.